



# Use of threshold parameter variation for tropical cyclone tracking

Bernhard M. Enz<sup>1,★</sup>, Jan P. Engelmann<sup>1,2,★</sup>, and Ulrike Lohmann<sup>1</sup>

<sup>1</sup>Institute for Atmosphere and Climate Science, Swiss Federal Institute of Technology, Zurich, Switzerland

<sup>2</sup>Institute of Computational Biology, Helmholtz Center Munich, Munich, Germany

★These authors contributed equally to this work.

**Correspondence:** Bernhard M. Enz (bernhard.enz@env.ethz.ch)

Received: 17 November 2022 – Discussion started: 12 December 2022

Revised: 10 July 2023 – Accepted: 17 July 2023 – Published: 6 September 2023

**Abstract.** Assessing the capacity of numerical models to produce viable tropical cyclones, as well as assessing the climatological behavior of simulated tropical cyclones, requires an objective tracking method. These make use of parameter thresholds to determine whether a detected feature, such as a vorticity maximum or a warm core, is strong enough to indicate a tropical cyclone. The choice of parameter thresholds is generally subjective. This study proposes and assesses the parallel use of many threshold parameter combinations, combining a number of weaker and stronger values. The tracking algorithm succeeds in tracking tropical cyclones within the model data, beginning at their aggregation stage or shortly thereafter and ending when they interact strongly with extratropical flow and transition into extratropical cyclones or when their warm core decays. The sensitivity of accumulated cyclone energy to tracking errors is assessed. Tracking errors include the faulty initial detection and termination of valid tropical cyclones and systems falsely identified as tropical cyclones. They are found to not significantly impact the accumulated cyclone energy. Thus, the tracking algorithm produces an adequate estimate of the accumulated cyclone energy within the underlying data.

## 1 Introduction

Numerical models are a useful tool to further our understanding of weather and climate as well as to make predictions thereof. Within these model simulations, certain features, like tropical cyclones (TCs), can be tracked and their behavior analyzed. TCs are of particular importance, as they pose an immense threat to human life and assets when they make

landfall. The damage caused by TCs is likely to increase with an increase in population and wealth in coastal areas (Pielke Jr. et al., 2008). Furthermore, Bender et al. (2010) predicted an increase in the frequency of category-4 and -5 hurricanes in a warmer climate, which is linked to an increase in destructiveness (Grinsted et al., 2019).

Model simulations, especially when performed with high horizontal resolution, for large domains, and for extended periods of simulated time, produce a vast number of output data. To analyze certain features, such as the lifetimes, intensities, and tracks of TCs, they must be identified. As manually tracking every TC is cumbersome, an automated and objective algorithm is preferable.

Any tracking algorithm implicitly contains a definition of the tracked system, and it then searches for instances where this definition is fulfilled. Within the context of TCs, a commonly used baseline is that a TC is a system with a maximum in vorticity collocated with (e.g., Chauvin et al., 2006) or in the vicinity of (e.g., Bengtsson et al., 1995; Zhao et al., 2009) a minimum in sea level pressure. The maximum in vorticity can be used without requiring the minimum in sea level pressure (e.g., Hodges, 1999). However, this alone does not distinguish TCs from other systems that can occur in the region of interest, such as extratropical cyclones (ETCs). Therefore, the warm-core structure of TCs is usually also searched for during the tracking process, which can be done directly or indirectly.

Directly assessing the warm core is done by defining a temperature anomaly, which compares the temperature at the TC center to that of the environment at a specified altitude or pressure. For example, Bengtsson et al. (1995) require the temperature anomaly at 300 hPa to be larger than that at 850 hPa while also requiring the sum of the temperature

anomalies at 300, 500, and 700 hPa to exceed a threshold value. This ensures that the temperature anomaly is stronger at higher altitude and that it is not too weak. Chauvin et al. (2006) require a strengthening of the temperature anomaly with height but only that the 700 and 300 hPa temperature anomalies exceed a threshold value. Zhao et al. (2009) use the mean temperature between 500 and 300 hPa to define the temperature anomaly, but they use the local maximum thereof, which must be within a  $2^\circ$  horizontal distance of the sea level. Indirectly assessing the warm core is done by searching for a pattern that is consistent with the presence of a warm core. For example, Bengtsson et al. (1995) and Chauvin et al. (2006) require the cyclonic wind to weaken with height, which is indirect evidence of a warm-core structure. Strachan et al. (2013) require that vorticity in the TC center is reduced with height, which is related to the weakening of cyclonic winds with height and, therefore, evidence of a warm core. Tsutsui and Kasahara (1996) detect the warm core by requiring the thickness of the 200–1000 hPa layer at the center and in the inner region of a TC to be larger than at the periphery. Walsh et al. (2012) combine the direct and indirect criteria, in that they require a positive 300 hPa temperature anomaly and a reduction in wind speed with height.

An alternative method of tracking TCs is provided by Tory et al. (2013), who used the Okubo–Weiss (OW) (Okubo, 1970; Weiss, 1991) parameter and absolute vorticity to form the OWZ parameter. The OWZ parameter reflects the solid-body component of absolute vorticity; thus, it can be used to identify vorticity-rich quasi-closed circulations. It is argued that every TC precursor shows increased OWZ, and thus the OWZ parameter is particularly useful to detect the early stages of a TC. Combined with vertical wind shear and relative humidity criteria, the OWZ parameter can then be used to track TCs (Tory et al., 2013; Bell et al., 2018). A review of TC tracking schemes can be found in Appendix B of Ullrich and Zarzycki (2017).

Many tracking criteria across many algorithms require that a system exceeds a corresponding threshold value. For example, the warm-core temperature anomaly must exceed the environmental temperature by a predetermined value or the central vorticity maximum must exceed a predetermined minimum value. This makes tracking algorithms inherently sensitive to the choice of these threshold values (Horn et al., 2014). If the threshold values are too weak, false positives may be found, and the algorithm cannot be trusted to detect only TCs. If the threshold values are too strict, TCs that exist in the model can be truncated in the early and late stages or missed entirely. Furthermore, the horizontal resolution of the model may affect how sensible a given threshold value choice is (Walsh et al., 2007).

While Horn et al. (2014) found that even small changes in threshold parameters can have a large impact on the tracking results, Zarzycki and Ullrich (2017) specify that the impact is large for the discrete count of TCs but relatively small for in-

tegrated metrics such as accumulated cyclone energy (ACE; Bell et al., 2000).

To make the tracking process less sensitive to the choice of threshold values, it is possible to vary these values. An example of this is provided by Camargo and Zebiak (2002), who use more strict threshold values to first identify TCs and then use relaxed threshold values forwards and backwards in time when a system is detected. This allows them to detect early and late stages of the TC life cycle with the relaxed values while mitigating the pitfall of falsely tracking non-TC systems.

The relative weakness of the defining TC characteristics at early and late stages in the TC life cycle is not the only complication to their tracking, as the existential question of when a TC begins and when it ends can also be asked outside of the scope of tracking. In the North Atlantic basin, only about 40 % of TCs form in the absence of baroclinic processes, and about 40 % of TCs form in a process called tropical transition (TT) (McTaggart-Cowan et al., 2013), where a precursor storm moves over warm water and attains TC characteristics (Davis and Bosart, 2003). Warm water is required because TCs form predominantly over water warmer than  $26^\circ\text{C}$  (Palmen, 1948), although TT events with a strong initial lower-level circulation can form at slightly lower sea surface temperatures (McTaggart-Cowan et al., 2015).

Montgomery and Smith (2014) describe the initial intensification of a weak cyclonic precursor system. They discuss how many mesoscale systems of deep convection, which they name vortical hot towers (VHTs), locally stretch vorticity within this precursor system, and how the thus produced cyclonic vorticity anomalies aggregate while the corresponding anticyclonic anomalies move outwards. This process gradually increases the vorticity of the precursor system and allows it to develop into a mature TC.

The termination of a TC can occur quite rapidly when they move over land. Other than this rather straightforward termination, there is also the possibility for a TC to develop characteristics of extratropical cyclones in a process called extratropical transition (ETT) (Evans and Hart, 2003). ETT occurs when a TC moves poleward and encounters a strong meridional temperature gradient, which enables it to form fronts and thereby strong radial asymmetry. This loss of symmetry and the increased vertical wind shear associated with horizontal temperature gradients cause the warm core to decay, such that the system develops an ETC structure. ETT occurs for 46 % of TCs in the North Atlantic basin, and transitioning systems account for about half of the systems that make landfall (Hart and Evans, 2001).

Both the initial and final stages of TCs are, therefore, not instantaneous but rather processes that take a finite amount of time to conclude. Thus, a tracking algorithm would preferably detect a cyclone at some point during its development and would cease to detect it at some point during its termination, as this would capture the entire TC phase of the cyclone

while allowing for some leeway during the phases immediately before and after.

While publications typically contain a description of how TCs are tracked, it is by no means common that they include an assessment of how well the tracking algorithm performs. As this is a fundamental component on which the data analysis builds, this paper is devoted to introducing a newly developed algorithm and assessing how well it performs. The new algorithm uses varying threshold values, which allows it to contain both lax and strict threshold value combinations, which are then combined to form a final tracking product.

The remainder of this paper is structured as follows: Sect. 2 describes the data and methods used to produce model TCs that can then be tracked, and it also presents the tracking algorithm; Sect. 3 shows that the numerical simulations are capable of producing viable TC-like vortices; Sect. 4 assesses the stage at which model TCs are first tracked; Sect. 5 assesses the stage at which model TCs are last tracked and why they terminate; Sect. 6 explores false positives and how they are caused; Sect. 7 assesses the impact of tracking errors on ACE; Sect. 8 assesses the sensitivity of the tracking process to the allowed translational velocity of TCs; and Sect. 9 summarizes the results and provides the drawn conclusions and an outlook.

## 2 Data and methods

### 2.1 Numerical simulations

The ICON model version 2.6.1 (Zängl et al., 2015) is used in limited area mode (ICON-LAM) to produce simulation data with which the tracking algorithm can be validated. ICON stands for “icosahedral, non-hydrostatic”, which refers to the icosahedral base grid with triangular grid cells that ICON uses and the use of non-hydrostatic equations. The simulation domain spans from the Equator to 70° N and from 120 to 15° W. An unstructured, triangular grid with a resolution of R03B07 (see Sect. 2.1 of Zängl et al., 2015, for more information on the grid nomenclature) is used, which corresponds to a grid spacing of about 13 km. A total of 50 vertical levels are used, with the distance between levels increasing with altitude. The first level is at about 10 m above the surface, and the model top is at 23 km. A time step of 100 s is used. Shallow and deep convection parametrizations are used (Bechtold et al., 2008). An ensemble of 20 members spanning the entire North Atlantic hurricane season is generated for the 2013 season. Within this study, this season is defined as beginning at 00:00 UTC on 1 June and ending at 00:00 UTC on 1 December. The month of May is used to initialize and spin up the simulations, as described below.

ERA5 data (Hersbach et al., 2020) are used to construct the initial state of the simulations, to prescribe monthly mean values for sea surface temperature and sea ice, and as lateral boundary conditions at 6-hourly intervals. Sea surface tem-

perature, sea ice, and boundary conditions are interpolated to individual time steps throughout the simulation. The physical fields that are prescribed at the boundary are zonal, meridional, and vertical wind; the logarithm of sea level pressure; temperature; specific humidity; cloud liquid water content; cloud ice water content; rainwater content; snow water content; and surface geopotential height. The first member of the ensemble is initialized at 00:00 UTC on 1 May 2013. The following 19 members have their initial times shifted by 24 h for each additional member, such that the final member is initialized at 00:00 UTC on 20 May 2013.

Even though the simulations are performed based on data for 2013, the TC activity in the simulations differs strongly from observations. As the intended focus of the study is on the validation of the tracking algorithm, and only a single season is simulated, a comparison of simulated data to observations is intentionally omitted. The intent of the numerical simulations is not to validate the ability of the simulations to reproduce the 2013 North Atlantic hurricane season but rather to produce a number of viable model-generated TCs that serve as the basis to validate the tracking algorithm. Thus, the simulated data can, for the focal purpose, be regarded as arbitrary manifestations of some TC season within which viable TCs exist and can be tracked.

### 2.2 Tropical cyclone tracking and evaluation

The tracking algorithm is based on that of Kleppek et al. (2008), which has previously been adapted to identify TCs in the ECHAM model output data. New features of the presented algorithm are the inclusion of a warm-core criterion as well as parallelization and threshold variation to address the threshold choice issue mentioned in Sect. 1.

The tracking algorithm requires mean sea level pressure, the vertical component of relative vorticity, and temperature on the 300 hPa isobaric surface on a regular longitude–latitude grid. For the purposes of this study, the chosen resolution is  $0.125^\circ \times 0.125^\circ$ , corresponding to about 14 km at the Equator, to which the ICON output is remapped. Vertical vorticity is used not on a pressure level, as ICON internally uses model levels. Over the ocean, these are at a constant geometric height; thus, vertical vorticity is used at 2.5 km, which corresponds to roughly 750 hPa. While this may seem odd, it should be noted that variations in the vertical vorticity threshold barely show any impact on the tracking process, as is argued later on. The main purpose of the vorticity criterion is to ensure that the rotation of the system is cyclonic.

Initially, all points on the horizontal grid are potential centers of a TC, and the algorithm then excludes all points that do not meet the criteria mentioned below. All points that remain are considered to be TC centers at this stage. This is done for each time step individually, such that no tracks are constructed at this stage. The following criteria need to be fulfilled for a point to qualify as a potential TC center, with the used values listed in Table 1:

**Table 1.** Threshold parameter values used in tropical cyclone tracking.

| Variable                   | Threshold values |           |     |      |     |
|----------------------------|------------------|-----------|-----|------|-----|
| $p_{s,dis}$ [km]           | 50               | 100       | 150 |      |     |
| $\zeta_{min}$ [ $s^{-1}$ ] | $10^{-6}$        | $10^{-5}$ |     |      |     |
| $\Delta T_{core}$ [K]      | 0.5              | 0.75      | 1   | 1.25 | 1.5 |
| $T_{dis}$ [km]             | 50               | 100       | 200 | 300  | 400 |

1. The sea level pressure must exhibit a local minimum within a given distance ( $p_{s,dis}$ ).
2. The vertical component of relative vorticity must exceed a threshold value within the lower troposphere ( $\zeta_{min}$ ).
3. The 300 hPa temperature directly above the sea level pressure minimum must exceed the mean 300 hPa temperature within a given distance ( $T_{dis}$ ) by a certain value ( $\Delta T_{core}$ ).

The algorithm evaluates these criteria in sequence, i.e., it identifies sea level pressure minima, the identified minima are subsequently evaluated for their vorticity, and the remaining points are then evaluated for their warm-core structure. All thresholds of this list are varied (see Table 1). This is done by prescribing not a single but multiple threshold values, and all threshold combinations are then used in parallel. This results in multiple distinct sets of identified TC centers that show considerable overlap, especially for strong TCs. Combinations with weak constraints identify weaker TCs more readily, whereas combinations with strong constraints identify only the stronger phases of TCs. This means that the tail ends of TCs are tracked by the weak constraints, whereas the strong constraints are less susceptible to falsely tracked points. The choice of threshold parameter values is based on parameters used throughout the scientific literature and on the physical feasibility of values (e.g., a positive value for the warm-core temperature difference that is within a range that can be exceeded by weak TCs). These choices are not tailored to the underlying dataset.

After TC centers at individual time steps are identified, tracks are constructed from them in a second step. To determine whether two TC centers at consecutive detection steps represent the same system, it is assumed that a TC can have a translational velocity of at most  $20 \text{ m s}^{-1}$ , which corresponds to  $1728 \text{ km d}^{-1}$ . The sensitivity to this velocity is explored in more detail in Sect. 8. If the two TC centers are within a distance that is consistent with this assumption, they are deemed to be the same TC. Tracks are only retained if they reach a minimum life time ( $\tau$ ). Within this study,  $\tau$  is always 18 h, meaning that a TC track must endure for at least four consecutive detection steps. The minimum life time criterion is necessary to remove very short-lived false positives that frequently occur well within the extratropics. These false pos-

itives are often a result of upper-level temperature gradients that are misidentified as warm cores.

This procedure results in a set of tracks for every parameter combination. These are then merged to form one final, singular set of tracks. To achieve this, every set is searched for instances of the same underlying TC, which typically has a variable track length because stronger constraints in the parameter thresholds produce shorter tracks than weaker constraints. As the tracking algorithm aims to include weaker phases, the full length of these tracks is retained. To exclude probable false positives, the number of parameter combinations that identified an individual TC, regardless of the individual track length, as long as the minimum life time is fulfilled, is considered. Tropical depressions (TDs; see Table 2) are very weak systems and are not easily identified. Thus, if 10 % of all combinations identify a TD, it is retained. Tropical storms (TSSs) are more intense, although still weak compared with hurricanes. They are retained if at least 20 % of all combinations identify the TS. Hurricanes are rather intense TCs and are, thus, comparatively easy to identify. They are retained if at least 50 % of all parameter combinations identify them. These values are subjectively chosen, based on visual inspection of azimuthally averaged wind and temperature fields of a subset of the considered TCs. While this introduces a fixed threshold again, the threshold value issue is reduced to one parameter, and this parameter does not describe the physical properties that the tracked system must exhibit.

The choice of the final parameter thresholds is tailored specifically to the underlying dataset. For use with other data, it is recommended that these values are revisited and adapted if necessary.

Because an important purpose of tracking TCs is to determine the activity within a season, the TC activity is quantified by the accumulated cyclone energy (ACE; Bell et al., 2000). It is calculated as the sum of the squared maximum wind speeds of all TCs at either the TS or hurricane stage at 6-hourly intervals, i.e.,

$$\text{ACE} = \sum_{i=1}^k v_{\max,i}^2, \quad (1)$$

where  $v_{\max}$  is the maximum wind speed of a TC at time  $i$ , which is documented every 6 h until the end of the season ( $k$ ). References to TC intensity follow the Saffir–Simpson Hurricane Wind Scale (Saffir, 1973), which has been slightly adapted to be consistent with commonly used modern values, as seen in Table 2. HURDAT2 data (Landsea and Franklin, 2013) are used to compare simulated ACE to observations.

The first and last detection steps of individual TCs are separated into a number of categories, which are described in Table 3. These categories aid in evaluating how early TCs are tracked and what causes them to terminate.

**Table 2.** The Saffir–Simpson Hurricane Wind Scale: TD is a tropical depression; TS is a tropical storm; Cat 1–Cat 5 are hurricane categories 1–5, respectively; and  $v_{\max}$  is the maximum instantaneous wind speed.

| Category | Maximum wind speed [ $\text{m s}^{-1}$ ] |            |            |    |    |
|----------|--|------------|------------|----|----|
| TD       |  | $v_{\max}$ | <          | 17 |    |
| TS       | 17                                       | $\leq$     | $v_{\max}$ | <  | 33 |
| Cat 1    | 33                                       | $\leq$     | $v_{\max}$ | <  | 43 |
| Cat 2    | 43                                       | $\leq$     | $v_{\max}$ | <  | 50 |
| Cat 3    | 50                                       | $\leq$     | $v_{\max}$ | <  | 58 |
| Cat 4    | 58                                       | $\leq$     | $v_{\max}$ | <  | 70 |
| Cat 5    | 70                                       | $\leq$     | $v_{\max}$ |    |    |

### 3 Tropical cyclones in the simulation data

Validation of a TC tracking algorithm requires that the model producing the underlying data can represent viable TCs, at least to the extent that the features used in tracking are truly features of the simulated TC. Figure 1 shows the azimuthal mean radial and vertical wind and temperature anomaly of the most intense TC within the dataset, which was a category-4 TC. The reference temperatures to determine the temperature anomaly comprise the azimuthal mean vertical profile at 500 km distance from the center. The third row of Fig. 1 shows the TC at its highest intensity, and the second and first rows show the TC 24 and 48 h prior to this, respectively.

The radial wind panels at all three aforementioned times show inflow within the boundary layer and outflow near the tropopause. This is a well-documented feature, which has already been reproduced by very early numerical simulations, where the boundary inflow is recognized as a feature crucial to the TC (e.g., Ooyama, 1969). The boundary layer inflow is rather weak in comparison to that found in Fig. 2 of Montgomery and Smith (2017); however, as this is not immediately relevant to the tracking algorithm, this is not investigated further. An expected feature, though absent from our simulated TC, is a shallow region of outflow above the boundary layer (Smith and Montgomery, 2015), as supergradient wind is lifted above the boundary layer and adjusts to gradient wind balance. A further feature of radial wind that is expected following Willoughby (1988), although it is absent in our simulated TC, is weak inflow throughout the mid-troposphere, which is linked to vortex stretching and, thus, TC intensification. Vortex stretching is also linked to changes in vertical velocity with height. All three vertical wind panels show clear updraft regions throughout the vertical extent of the troposphere, beginning at a radius of about 50 km near the top of the boundary layer. The vertical wind speed increases with height in parts of this updraft region, which is indicative of vortex stretching. In particular, the panel at 24 h before maximum intensity in Fig. 1 shows a deep region of an increase in vertical velocity with height, which is reversed at a height of around 11 km. This reversal leads to a reduction

in vorticity, which manifests itself as a reduction in tangential velocity (not shown), and is collocated with the outflow region. Thus, the missing mid-level inflow is not indicative of absent vortex stretching, as the vertical wind profile shows clear signs of vortex stretching. The eye of a well-developed TC is characterized by subsidence, as shown in Montgomery and Smith (2017) for simulated TCs. While this is present at the time of maximum intensity, it is not present 24 h earlier nor well developed 48 h earlier. Possible causes for this are the general weakness of the subsidence as well as the small scale of this phenomenon. Furthermore, it has been found that increasing the horizontal resolution of numerical simulations beyond the resolution used in this study can affect the range of downdraft velocities (Gentry and Lackmann, 2010). Generally, the numerical simulations within this study have the capacity to produce the mean secondary circulation features of TCs rather well, even if the more intricate features of secondary inflow are not represented well. Notably, the numerical model can produce vortex stretching in the lower troposphere, which is relevant to the tracking algorithm because it requires a vorticity maximum.

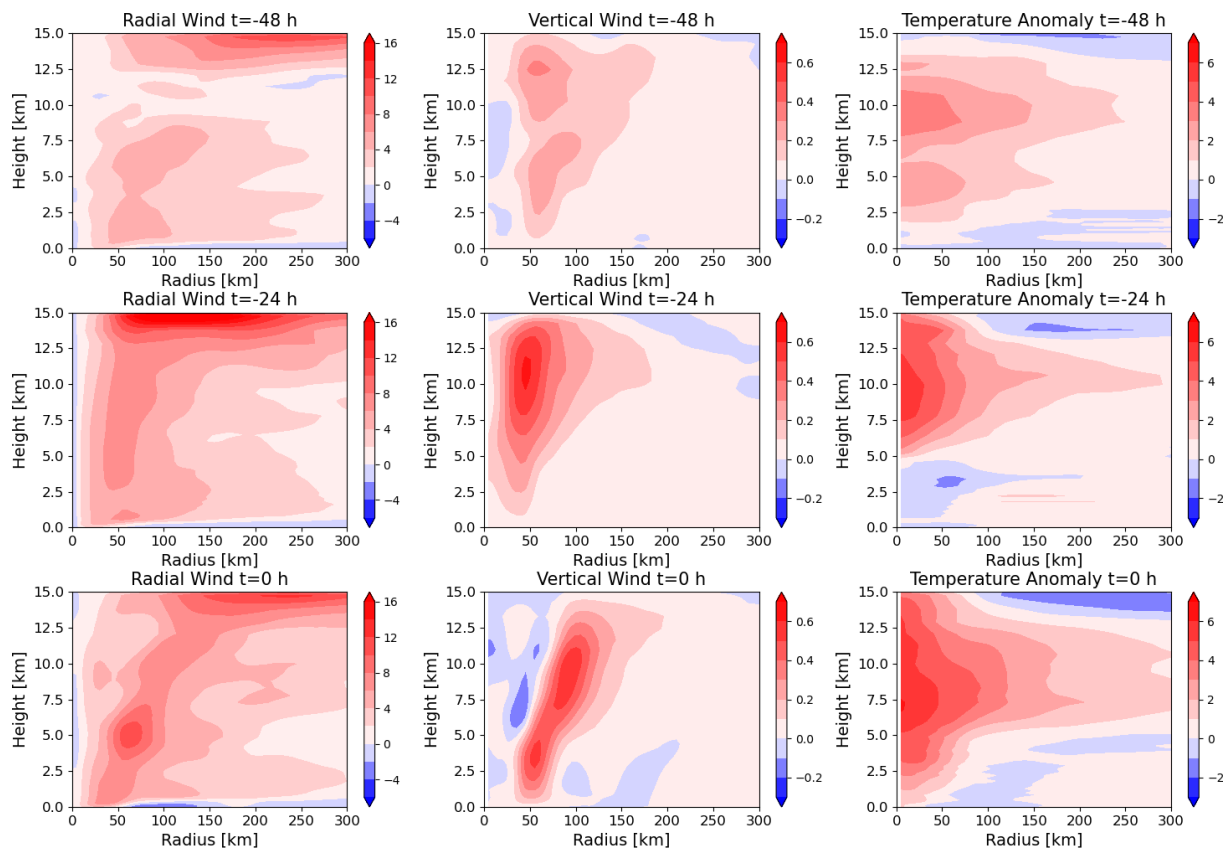
The temperature anomaly panels for all three time steps in Fig. 1 show a distinct warm core at the center of the TC. The magnitude of the anomaly increases with increasing TC intensity, which is consistent with the findings of Durden (2013), and the temperature anomaly maxima fall within the height range of 760–250 hPa described therein. As is discussed in Stern and Nolan (2012), the altitude of the warm core can vary drastically, and multiple local maxima can coexist. They find that the most common altitude for the strongest warm-core maximum is between 4 and 8 km. Wang and Jiang (2019) found that the height of the warm-core maximum increases with TC intensity and typically ranges from 10 to 11 km for category-4 TCs. Therefore, the shown TC has a warm core at an acceptable height. It is, thus, concluded that the numerical simulations have the capacity to produce warm-core features that the tracking algorithm requires to distinguish tropical cyclones from extratropical cyclones.

Figure 2 shows all TCs of a single ensemble member, indicating their category and the percentage of parameter combinations that detected a given track segment. Tracks typically start at very low intensities and with a lower percentage of threshold parameters detecting the system. The TS and hurricane stages are detected by more parameter combinations, as their structure is more developed. The parameter combinations with weaker constraints are therefore necessary to capture the early stages of TCs.

Figure 3 shows the accumulation of ACE throughout the season for HURDAT2 data and for the 20 simulated ensemble members. While the simulations underestimate the TC activity early in the season, this is compensated for by high activity during September, where most of the activity is concentrated. While most simulations eventually drastically overestimate ACE, it is important to note that the 2013 season was one of very low activity (see, e.g., Zhang et al., 2016,

**Table 3.** Description of genesis and termination categories with the occurrence rate of each category. The total number of tracked TCs is 113, and about 12 % of tracked TCs are false positives. Not all terminations fall under this categorization.

| Category                   | Occurrence | Description   |
|----------------------------|------------|---|
| Genesis categories         |            |   |
| Single maximum             | 36 %       | TCs exhibit a single vorticity maximum near the central sea level pressure minimum or present only very weak secondary maxima around a strong central maximum within the first 24 h.  |
| Transitional               | 34 %       | TCs exhibit multiple vorticity maxima near the central sea level pressure minimum and transition to a single vorticity maximum, possibly with very weak local maxima around a strong central maximum, within 24 h of first detection. |
| Multiple maxima            | 19 %       | TCs exhibit multiple vorticity maxima near the central sea level pressure minimum within the first 24 h.  |
| Termination categories     |            |   |
| Warm-core offset           | 52 %       | The warm-core offset relative to the central pressure minimum becomes too large to fulfill the warm-core criteria.  |
| Translation velocity       | 27 %       | The translational velocity becomes too large for the algorithm to continue the constructed track.   |
| Vanishing pressure minimum | 4 %        | The central pressure minimum vanishes and, thus, there is no local minimum to be tracked any longer.  |



**Figure 1.** Azimuthal mean radial wind (first column), vertical wind (second column), and temperature anomaly (third column) of the most intense TC within the simulation dataset at its highest intensity (third row) and 24 h (second row) and 48 h (first row) prior.

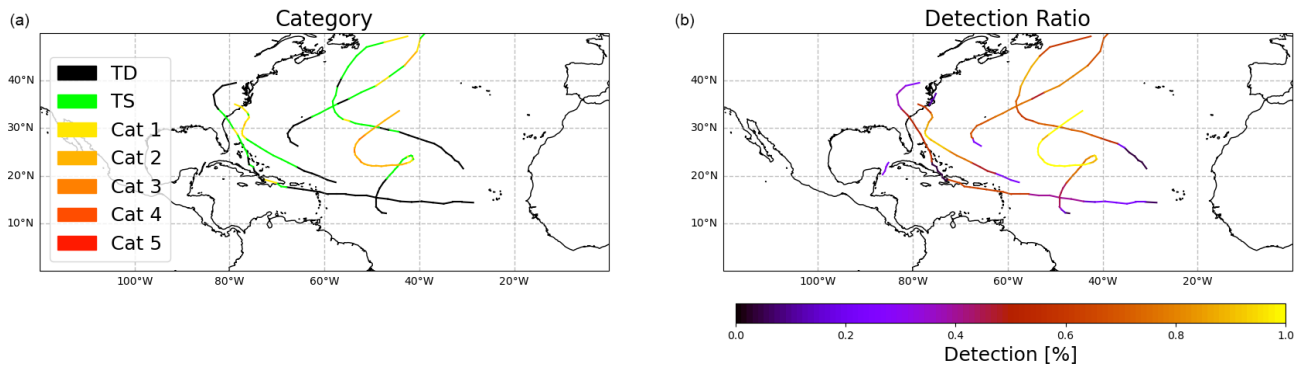


**Figure 2.** Tropical cyclones detected in a single ensemble member. Panel (a) shows their category, and panel (b) shows the percentage of parameter combinations that detected a given track segment.

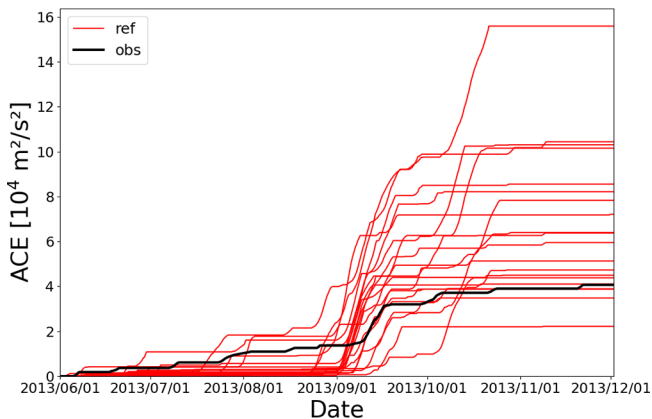


**Figure 3.** Accumulation of ACE throughout the season for HURDAT2 data (black) and the 20 simulation ensemble members (red).

for a discussion of the low activity and its causes). Overall, the simulations produce ACE values that are realistic compared to observed TC seasons, although not necessarily for the 2013 season. Thus, in terms of ACE, they can be used to represent arbitrary TC seasons, as intended.

#### 4 Genesis detection

The detection of tropical cyclogenesis is met with a fundamental problem: TCs typically form from a pre-existing disturbance that gradually develops TC-like characteristics. This means that there is no clear distinction between the pre-existing disturbance and the developed TC. As the tracking algorithm aims to maximize the duration of a TC, how early a TC is detected is sensitive to how weak the most liberal threshold values are chosen. Hence, it is of interest to investigate how early in the life cycle of a TC the system is detected.

For all detected TCs, the first tracked 24 h are divided into the three genesis categories listed in Table 3. As the number of TCs is not prohibitively high, this division is done manu-

ally to avoid possible oddities in the categorization that an algorithm could produce, although it does introduce some subjectivity. A total of 113 TCs across 20 ensemble members (i.e., about 5–6 TCs per simulation) are assessed, of which about 12 % are false positives (as discussed in Sect. 6). Figs. 4–6 show a detection percentage, which is the number of parameter combinations that identified the specific TC at the given time. The maximum of this percentage along the entire track is what the algorithm uses to decide whether a track is retained. The figures show the temporal evolution of this percentage throughout the first few time steps.

Figure 4 shows a typical example of the single-maximum category. This category requires a TC to exhibit a single vorticity maximum near the central sea level pressure minimum or to have only very weak local vorticity maxima around a strong maximum throughout the entire 24 h period. About 36 % of all tracked systems fall within this category. The horizontal wind speed panels show an asymmetry in the cyclonic wind, which is due to the superposition of the cyclonic wind field and the translational velocity of the TC. Furthermore, the wind speed at the center of the TC is very low, which is a result of the vanishing tangential wind speed towards the center. Thus, the TC has a developed cyclonic circulation. The vorticity panels, as per the categorization, show a strong central maximum with comparatively very weak local maxima in the vicinity. The lack of a tracked aggregation phase is not necessarily indicative of a flaw in the tracking algorithm, as TCs can be generated from an extratropical precursor cyclone via TT (Davis and Bosart, 2004), where the precursor cyclone attains TC characteristics. TT accounts for over a third of cyclogenesis events in the North Atlantic (McTaggart-Cowan et al., 2013). The algorithm only tracks these cyclones once the TC characteristics are sufficiently developed. This underlines the importance of the warm-core criteria, which serve to distinguish ETCs from TCs. The temperature anomaly panels show a distinct warm core very close to the center in all three instances. After 24 h, the warm core is offset to the southeast of the TC center. While the offset is not immediately relevant to first detection, it shows



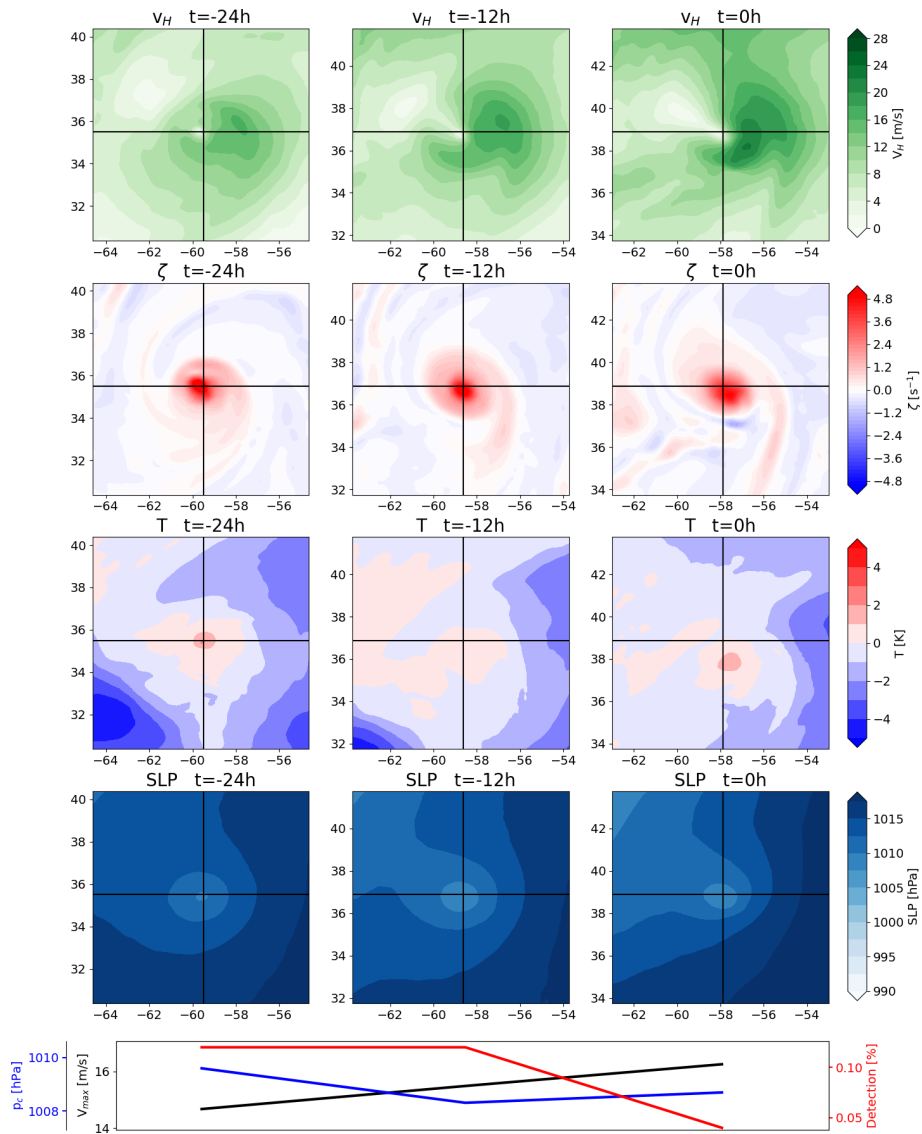
that the warm-core criteria allow for some offset of the warm core relative to the TC center without losing the ability to track the TC. The allowance for this displacement is sensitive to the warm-core threshold parameters, which is reflected in the reduction in the detection percentage for this time step, in that the percentage is decreased for a more intense but also more offset core. This, in turn, shows that the detection percentage is not sensitive to TC intensity alone. The mean sea level pressure panels serve to show that the algorithm tracks a genuine low-pressure system, not a spurious local minimum. Notably, the low-pressure system is still tracked when it is embedded in a larger-scale pressure gradient, underlining the importance of a parameter that defines the region within which a point must constitute a local minimum.

Figure 5 shows a good example of the transitional category, in that the first time step shows a number of local vorticity maxima of roughly equal magnitude spread throughout a sizable region. This category requires that, at first detection, there are multiple local vorticity maxima in the vicinity of the central mean sea level pressure minimum. Within 24 h, these must give way to a single vorticity maximum, possibly with comparatively very weak local maxima around it (i.e., it must transition into the pattern that the single-maximum category requires from first detection on). Thus, this category captures TCs that complete an aggregation phase of mesoscale convective systems within the first 24 h of detection. About 34 % of all tracked systems fall within this category. A good example of this category is shown instead of a typical example for two reasons: first, this shows the situation that the variation in parameters aims to track more effectively; second, the panels 12 h after first detection show a situation that is reflective of a typical first detection in this category, such that a more typical situation is still captured by the figure. The wind field panels show a pattern similar to that of the previous category, where cyclonic flow is enhanced in the direction of translation and reduced in the opposing direction. The location where the tangential velocity is drastically reduced close to the center is slightly offset from the mean sea level pressure minimum, which is typical of the tracked TCs within this category. Once the transition to a single vorticity maximum is completed, this offset typically becomes very small or vanishes entirely. The vorticity panels show many local maxima of comparable intensity at first detection. In this stage, a key component of the production of vertical relative vorticity is the stretching of pre-existing vertical vorticity. Examination of the vertical wind speeds shows that the vorticity maxima are located where the vertical wind speed increases with height (not shown), which strongly suggests the presence of vortical hot towers, as discussed in Montgomery and Smith (2014), or, at the very least, the strong generation of vertical vorticity through vortex stretching. Therefore, the algorithm appears to be tracking the aggregation stage of mesoscale systems, which then develop into a TC. Thus, the algorithm successfully fulfills the goal of capturing this stage for about a third of all tracked systems. However, this stage is typically

only detected when the aggregation has progressed substantially, as the panels depicting the TC 12 h after first detection are more typical of this category. The warm core intensifies throughout the aggregation period, and the location of the maximal temperature anomaly moves closer towards the center of the TC. These two factors cause the detection percentage to increase drastically from the first to the second panel. This shows that the early aggregation phase is within a range where the warm-core parameters are crucial to detection and the thermal structure of the TC must show some organization. The sea level pressure panels show that the algorithm can track low-pressure systems that are rather weak, as is required for capturing the aggregation phase. The maximum wind speed at first detection is close to TS strength in this example, but it can be around  $10 \text{ m s}^{-1}$  in other examples. This low maximum wind speed reflects the early detection in the non-aggregated state. The maximum wind speed as tracked by the algorithm is not identical to the maximum wind speed seen in the figure. This is because the algorithm only searches for the maximum wind speed within 100 km of the TC center to ensure that there is no false inclusion of winds outside of the TC circulation. The maximum wind speed can therefore be underestimated for TCs with a very large radius of maximum winds. Hence, this constraint on the maximum radius of maximum winds should be revisited for use with other datasets.

Figure 6 shows a typical example of the multiple-maxima category. This category requires that there are multiple vorticity maxima throughout the first 24 h of the TC and that there is no singular maximum that is substantially stronger than the others. About 19 % of all tracked systems fall into this category. The wind field panels differ substantially from those shown for the previous two categories. While the very low wind speeds at the center still indicate cyclonic rotation, this is not evident from the winds further away from the center. Thus, the cyclonic rotation is rather weak and is obscured by environmental winds. This calls the usefulness of a maximum wind speed metric into question, but it will be shown below that these early phases barely impact ACE. This particular example develops into a category-1 hurricane about 1 week later, which has a much larger impact on ACE. The vorticity panels show only few vorticity maxima, but these increase in number throughout the first 24 h. This could be due to more VHTs forming, which locally stretch vorticity and aggregate later on. This implies that TCs of this category are detected very early in their life cycle, which is intended. The warm core is barely developed at first, but it intensifies throughout the first 24 h. However, there is no single central maximum but rather a few local maxima emerge. This unstructured warm core is reflected in the detection percentage, which is barely high enough to not discard this stage of the life cycle. The warm-core criteria are, thus, capable of detecting systems early on, but they are not liberal enough to track any low-pressure system with mild diabatic heating. It appears that a substantial region of increased temperature is





**Figure 4.** Example of a TC in the single-maximum genesis category, presenting the 850 hPa horizontal wind magnitude (first row), 850 hPa vertical vorticity (second row), 300 hPa temperature anomaly (third row), mean sea level pressure (fourth row) and central pressure (blue), maximum wind speed (black), and detection percentage (red) at the three times shown (fifth row). The first column depicts first detection, the second column shows the TC 12 h after first detection, and the third column shows the TC 24 h after first detection. The black crosshairs indicate the TC center.

required for the tracking algorithm to detect a TC, especially when the increased temperature is offset relative to the TC center.

### 5 Tropical cyclone termination

The termination of a TC is, much like genesis, not strictly defined. Therefore, the following points are investigated: (i) what the tracking algorithm deems to be the last time step at which a TC exists and (ii) why it is not tracked further. The algorithm ceases to track a system when the surface pressure minimum disappears, vorticity becomes too weak, the warm

core can no longer be detected, or the translational velocity is too large to construct a track. Only one of these circumstances needs to occur for the track to be terminated. Within the dataset used, three main causes for TC termination have emerged: (i) the TCs either have a warm core that is offset in a way that increases the environmental temperature such that the warm-core criterion is no longer fulfilled, (ii) the warm core weakens substantially, or (iii) the TC moves too fast to be connected to previous detection steps. Typically, at least two of these processes occur in parallel. Figures 7 and 8 resemble those of the previous section, but they now span only the last 6 h of the TC in the first and second col-

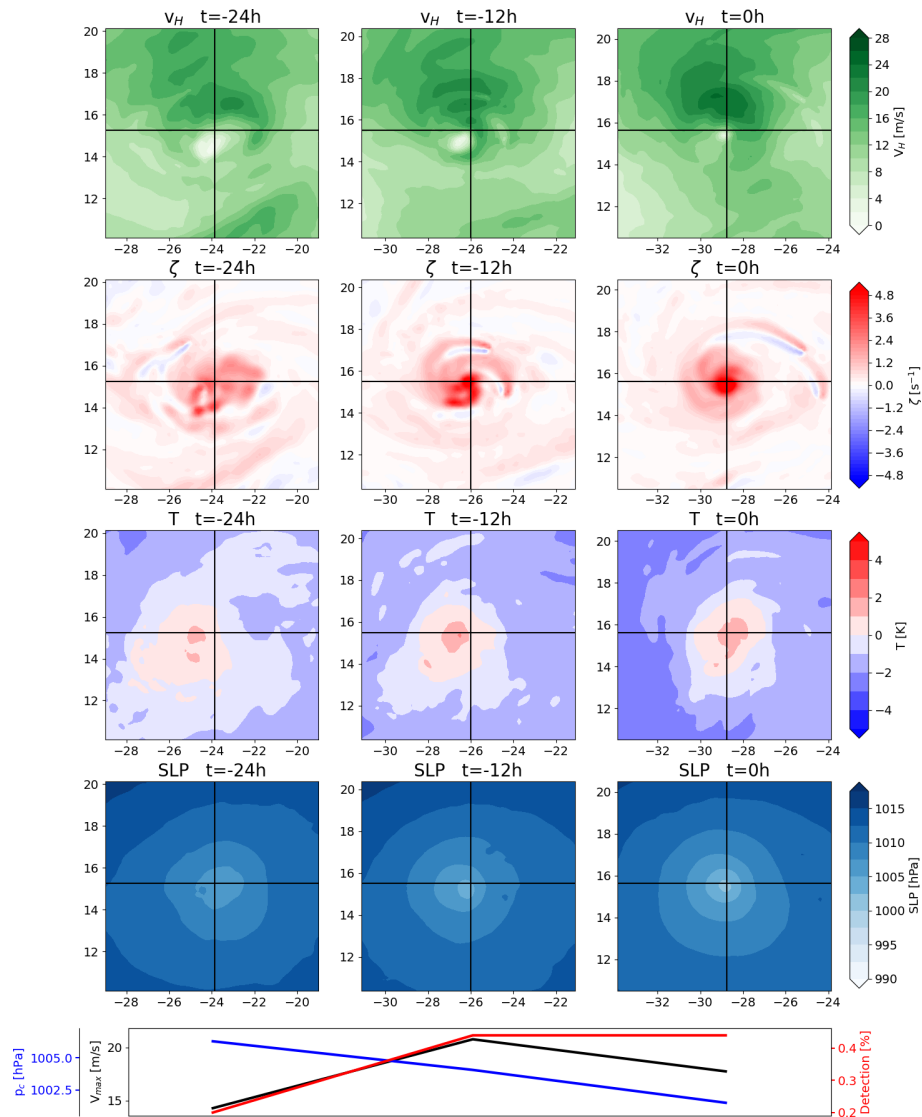


**Figure 5.** Same as Fig. 4 but for a TC in the transitional genesis category.

umn, and the third column shows plots 6 h after the TC is last tracked, centered on the final TC position. Mean sea level pressure contours are overlaid on the horizontal wind magnitude, the vorticity, and the temperature anomaly to better identify where the pressure minimum is located relative to features within these plots. The temperature anomaly within the figure (not during the actual tracking) is calculated using a  $4^\circ \times 4^\circ$  square centered on the center of the crosshairs as a reference, as this is somewhat reflective of how the temperature anomaly is calculated by the tracking algorithm.

Figure 7 shows an example of a TC where the tracking algorithm finds a pressure minimum with sufficient vorticity but where the warm core is offset relative to the pressure minimum and is weakening in intensity. The wind magnitude panels show a cyclonic wind field around a pressure minimum even after the TC is no longer tracked, and the vorticity

panels show that there is sufficient vorticity to fulfill the vorticity criterion at all times. In the third column, the distance between the pressure minimum and the last tracked position is also well within the permissible distance that would allow for a track to be constructed. Therefore, the TC must be terminated by the warm-core criteria no longer being fulfilled. This is because the weakening warm core is positioned east-southeast of the pressure minimum and some distance away from it. Thus, the pressure minimum is located towards the edge of the warm core. This combines a rather weak anomaly above the pressure minimum with an environmental temperature that is heavily impacted by the presence of the warm core, such that no warm core is detected. The weakening warm core throughout this period is not directly visible in the figure because the reference temperature is progressively reduced, but the absolute temperature of the maximum does

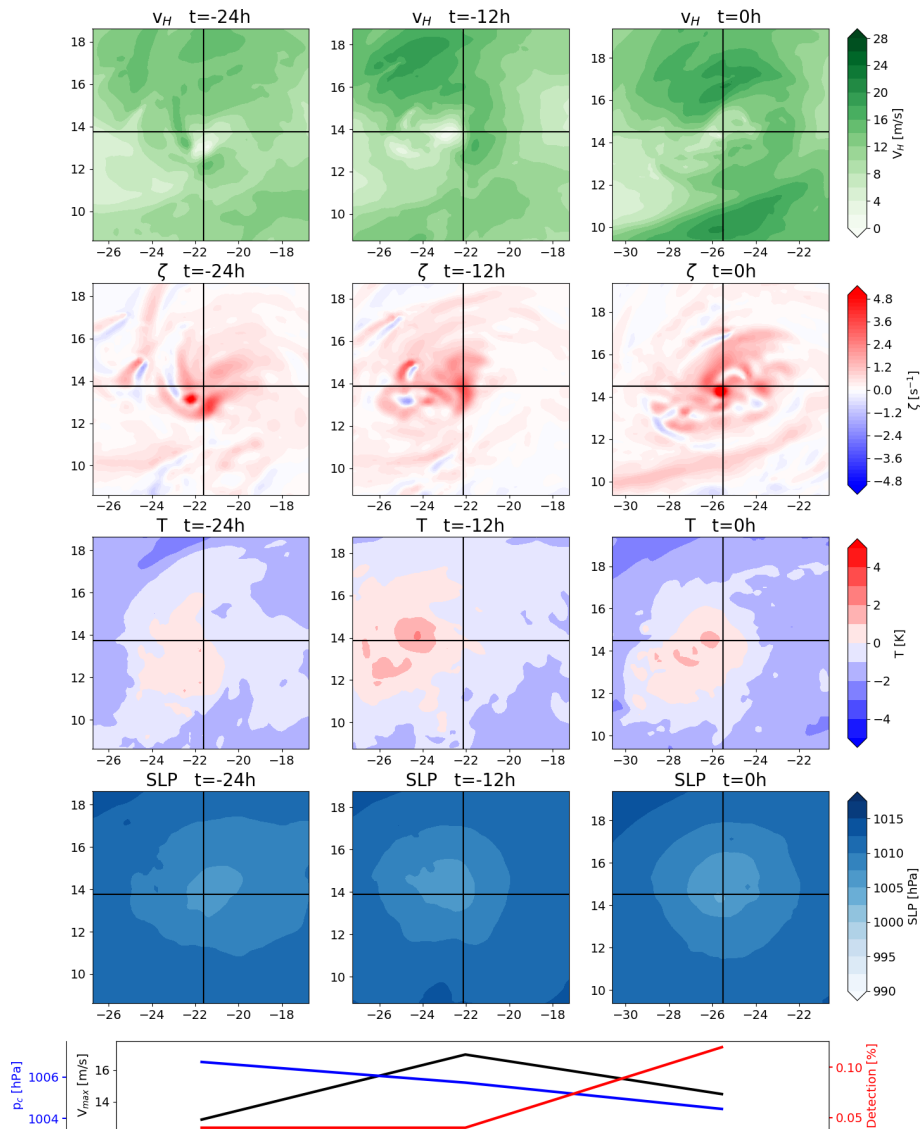
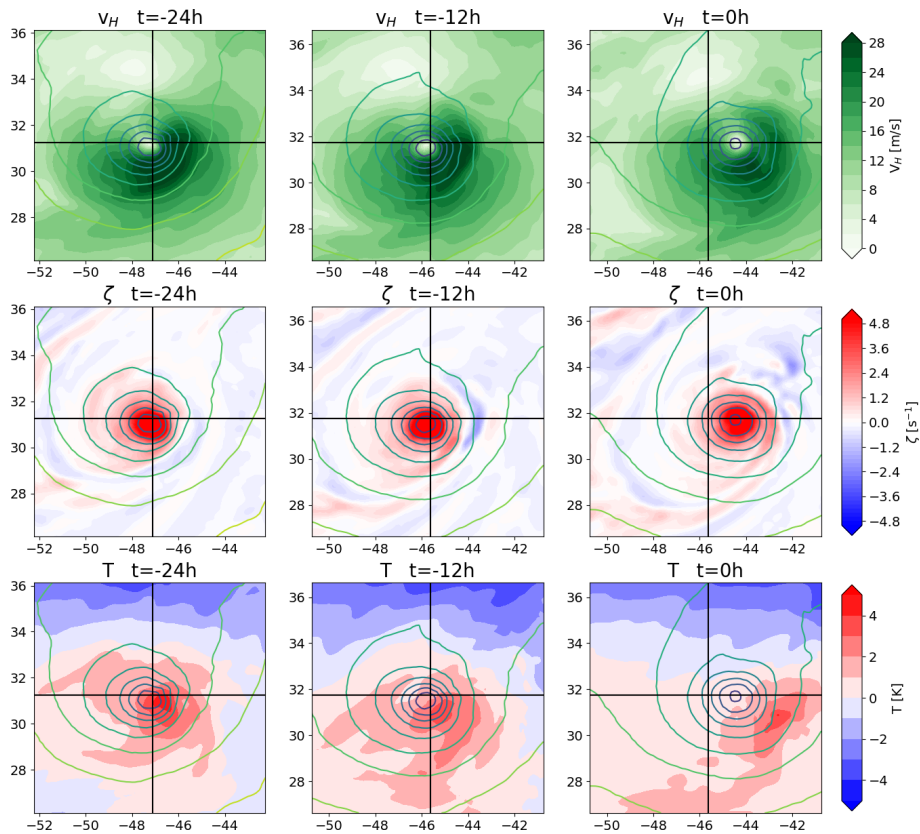


Figure 6. Same as Fig. 4 but for a TC in the multiple-maxima category.

indeed decrease and the area of elevated temperature decreases as well. This aids in offsetting the warm-core location from the pressure minimum, as the area of strong temperature anomaly is reduced. This scenario is the most common, with about 52 % of cases terminating due to an offset of the warm-core position.

Figure 8 shows an example where the TC has a translational velocity that is too large for a track to be constructed. While the TC moves about  $3^\circ$  to the north and  $2^\circ$  to the east between the last two tracked steps (translating to about 385 km at a velocity of  $18 \text{ m s}^{-1}$ ), it subsequently accelerates and moves about  $4^\circ$  to the north and  $3^\circ$  to the east, translating to about 500 km at a velocity between 20 and  $25 \text{ m s}^{-1}$ , making it too fast for a track to be constructed. The wind field panels indicate that there is still cyclonic rotation around a pressure minimum, and the vorticity panels show that there

is still strong vorticity associated with the TC. The warm-core criteria also seem to be fulfilled. However, a feature that is typical of such cases is that there is a strong environmental temperature gradient as well as cold air enveloping the TC in a cyclonic fashion. This is indicative of ETT (Evans and Hart, 2003), which may also be the cause of the increasing asymmetry in the vorticity field surrounding the TC. The intensity of the warm core is substantially reduced within the shown 12 h window, which is consistent with the erosion of a warm core during ETT. Therefore, it appears that TCs that have an overly high translational velocity tend to be TCs that are interacting with extratropical flow and are undergoing ETT. While it is reasonable to exclude transitioned TCs, the precise moment where tracking is terminated is not controllable with this algorithm. Furthermore, the tracks do not terminate explicitly because of the transition process but rather because



**Figure 7.** Example of a TC in the warm-core offset termination category, presenting the 850 hPa horizontal wind magnitude (first row), 850 hPa vertical vorticity (second row), and 300 hPa temperature anomaly (third row), with overlaid mean sea level pressure contour lines. The black crosshairs indicate the tracked TC center for the first two columns and the last tracked TC center (i.e., that of the second column) for the third column.

the TCs accelerate, making this termination scenario convenient but accidental. About 27 % of TCs terminate due to an overly large translational velocity.

For more control over the termination of a track (or continued tracking but with appropriate labeling) due to ETT, it may be beneficial to explicitly treat ETT. Bourdin et al. (2022) and Bieli et al. (2020) both describe methods based on the definition of ETT provided in Evans and Hart (2003) to distinguish between TCs and ETCs. The explicit treatment of ETT is currently not implemented in the scheme here, but it will be the focus of possible future improvements.

Far less common is the vanishing of the sea level pressure minimum. This occurs when a substantially larger low-pressure system absorbs the local pressure minimum, which causes the TC to weaken and its pressure minimum to vanish towards the edge of the larger low-pressure system. This is the case for four TCs within this dataset. There is one TC that approaches the eastern boundary of the domain at 15° W, where it weakens and is eventually no longer tracked. Due to the proximity to the boundary, it is not counted in any of the other categories.

In conclusion, tracked TCs reliably terminate due to the erosion or offset of the warm core, due to interaction with extratropical flow, or due to the vanishing local pressure minimum at their center. The translational velocity criterion aids in terminating TCs when they interact with extratropical flow, even when the warm core is still present. While this is convenient, as TCs terminated in this manner show strong asymmetry instead of the typical radial symmetry of a TC, it is not intended and is not controllable by parameter choice. The maximum translational velocity parameter serves to form tracks out of individual detection steps and must be chosen to fulfill that function. It can, therefore, not be chosen freely and adapted to optimize its function as a termination criterion.

## 6 False positives and other tracking issues

Naturally, there are limitations to the tracking algorithm. Other than beginning to track TCs too early or terminating them too late, there are also instances of tracked systems that cannot feasibly be considered TCs. About 12 % of all tracked systems are false positives. Almost all of these cases

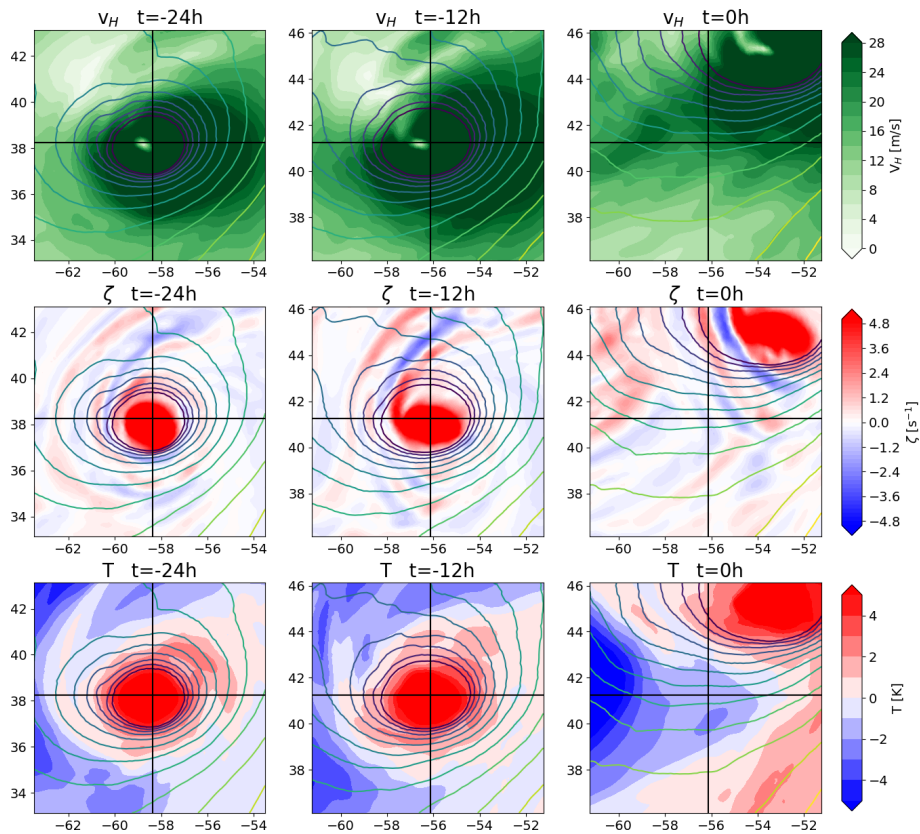


**Figure 8.** Same as Fig. 7 but for a TC in the translational velocity termination category.

show traits of extratropical cyclones; this is consistent with Bourdin et al. (2022), who found false alarms to frequently be caused by extratropical cyclones. Edge cases are mostly eliminated by the life time criterion of the algorithm. Figure 9 shows a typical example of such a case. The wind field at all shown times shows an elongated band of high wind speeds but no central minimum. There appears to be no discernible center of cyclonic flow near the track center, indicating that the wind field is inconsistent with the existence of a TC at this location. The vorticity fields at all shown times further substantiate this, as elongated bands, partially with alternating signs, are inconsistent with a developed TC and also inconsistent with the aggregation of local maxima caused by vorticity stretching as seen in previous examples. The temperature fields do not show warm cores but rather positive anomalies in an environment with a strong temperature gradient. The presence of strong negative anomalies reduces the environmental temperature sufficiently for the algorithm to detect what it believes to be a warm core, as the positive anomaly at the center does not need to be pronounced nor confined to a small region to be above the environmental mean temperature. The sea level pressure fields show that the center of the tracked system is not where the pressure minimum of the low-pressure system is located. Instead, the distance from the true pressure minimum of the system in-

creases with time. Thus, it is concluded that the algorithm can mistakenly track frontal structures in extratropical cyclones, as these can show a local pressure minimum, sufficient vorticity, and a strong temperature gradient that technically fulfills the warm-core criterion, even though it is not a true warm core. Other, atypical cases of false positives are local pressure minima with some positive vorticity that are in an environment with a strong temperature gradient, which fulfills the warm-core criterion even though no true warm core is present.

Outside of false positives, it is possible for the algorithm to detect a TC but to falsely identify first detection. Figure 10 shows a case where first detection is close to the TC's true location. At first detection, the minimum in the wind field that indicates the center of the cyclonic rotation is some distance away to the northeast, as is the vorticity maximum. As the vorticity maximum is rather broad and only a few spurious and comparatively weak local maxima are located outside of it, there appears to have been an aggregation phase prior to detection. The sea level pressure shows a minimum close to the wind speed minimum and a vorticity maximum to the northeast of the tracked center. In the following detection steps, the system is tracked correctly. This false tracking is likely caused by the pressure minimum to the northeast of the first detected point not fulfilling the warm-core criteria.



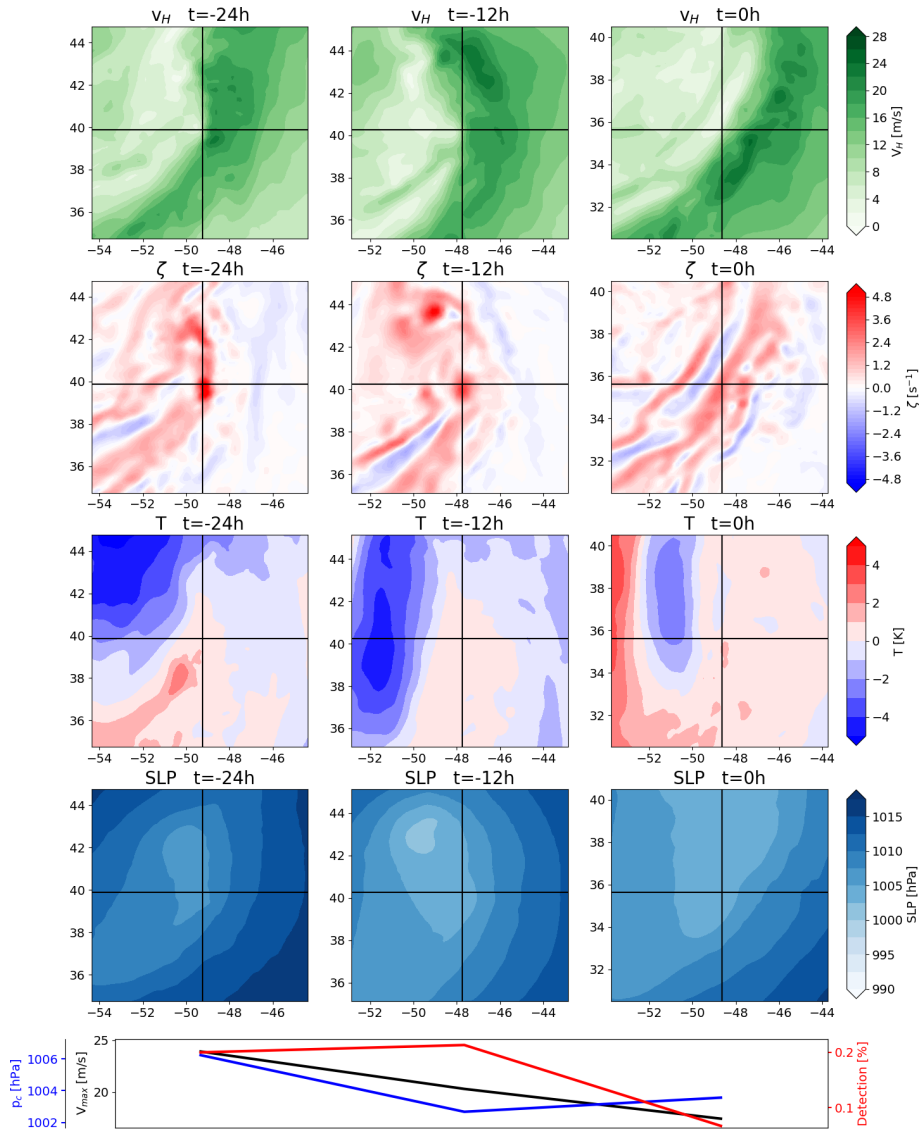


Figure 9. Same as Fig. 4 but showing a falsely tracked frontal structure.

A local minimum outside of this – the falsely tracked center – fulfills all criteria in what appears to be a single or at most two parameter combinations, as indicated by the very low detection percentage at this time. This falsely tracks a system earlier than it otherwise would be at a location that does not reflect where the system is located. It should be noted that this is the only case within this dataset where first detection of a TC is at the wrong location.

Similar to falsely identifying the beginning of a TC, it is possible for the algorithm to detect a TC correctly but to then not terminate it early enough. Figure 11 shows a case where a legitimate TC is detected, but the algorithm then detects a local pressure minimum adjacent to a stronger low-pressure system. This local minimum has sufficient vorticity to fulfill the threshold requirement and is in a region with a sizable temperature gradient. This allows the system to fulfill

the warm-core criterion without having a warm core, causing the algorithm to continue to track a system beyond ETT. Two such cases exist within the dataset used.

In conclusion, there are features tracked by the algorithm that are not TCs, and TCs are not always tracked correctly. False positives are rather rare (about 12 % of all tracked systems). The impact of these errors on ACE is explored in the following section.

### 7 Tracking error impact on ACE

Within this paper, the main metric used to describe tropical cyclone activity is ACE. To determine the effect of tracking errors on ACE, a few different ACE calculations are considered. Figure 12 shows box plots of the 20 ensemble members

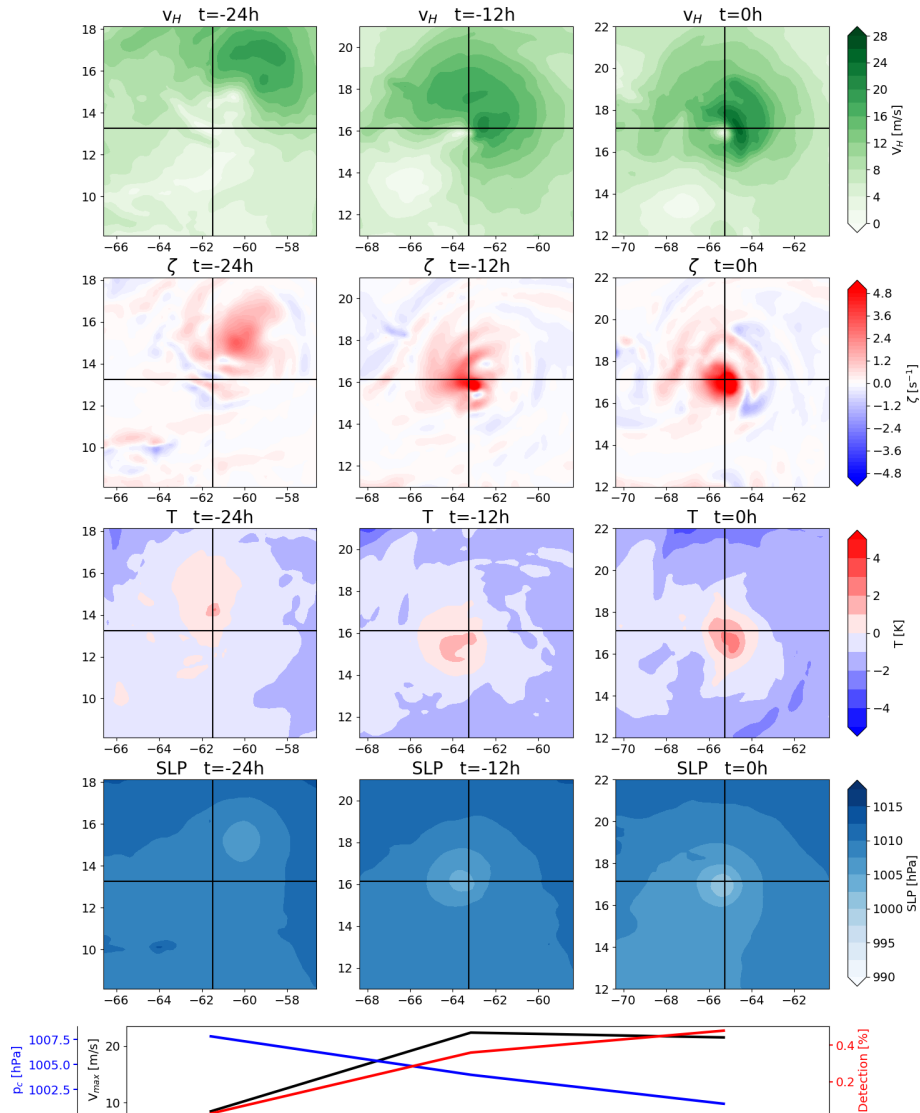


Figure 10. Same as Fig. 4 but showing a falsely tracked initial location.

and compares the different calculations. The first is full ACE, which includes all TCs at stages of TS strength or higher, including the false positives. This distribution is used as a reference for the following three. The second calculation is the same but excludes all manually identified false positives. A one-sided  $t$  test is performed to determine whether the distributions differ significantly, and the resulting  $p$  value is 0.54. Therefore, there is no significant effect on ACE when false positives are included in the calculation. This is likely because the identified false positives typically have short lifetimes and are not very intense; therefore, they do not substantially contribute to ACE.

The third calculation includes all TCs at stages of TD strength or higher. The underlying rationale is that extending the tail ends of the tracks and having varying track lengths depending on tracking parameter threshold choices could im-

part the energy produced by individual TCs, which would not be captured by the regular ACE calculation. However, a one-sided  $t$  test yields a  $p$  value of 0.43, which shows that no significant difference is produced by the inclusion of the TD stage. Thus, the track extension of the parameter combinations with weak constraints allow for very early stages in TC development to be tracked without significantly affecting the energy produced by individual TCs.

The fourth calculation only includes the hurricane stage of TCs. This is done to show that extending the tail ends of TCs does not significantly impact the ACE contribution of individual TCs. In principle, the algorithm could extend the lifetime of TCs for too long or could track them too early. As shown previously, this could be an issue when ETT and TT are involved, as there is no explicit treatment of these processes. Removing all TS-stage data from ACE is an estimate



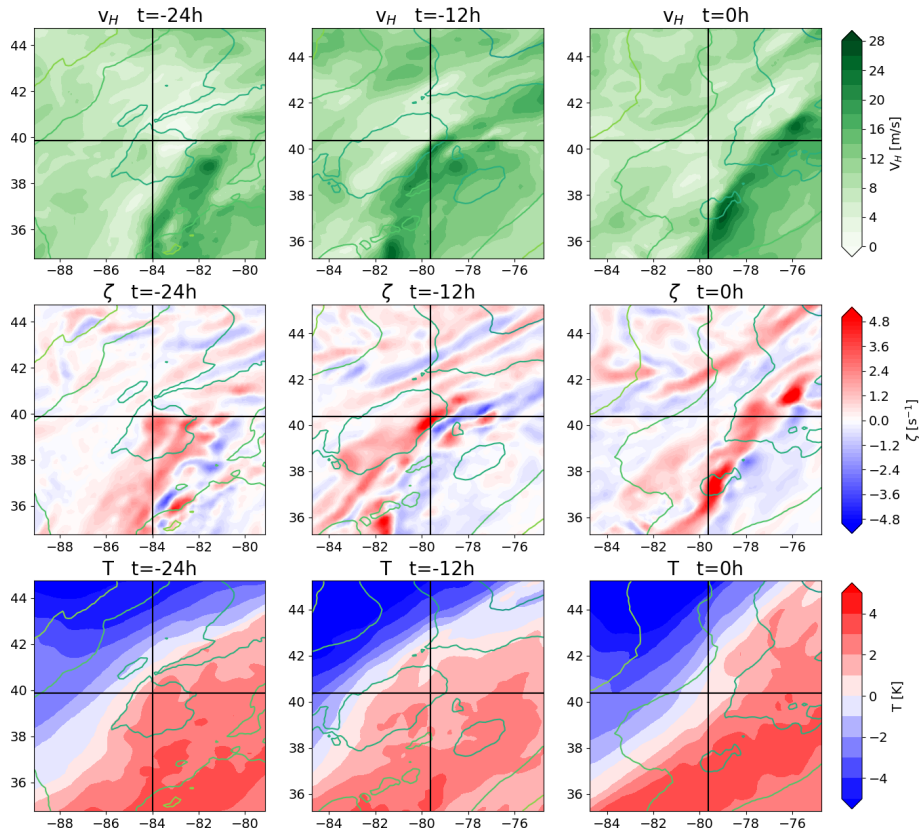


Figure 11. Same as Fig. 7 but showing a false continuation of a TC that no longer exists.

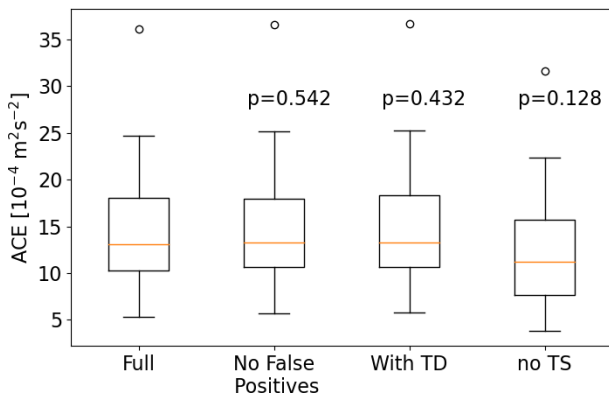


Figure 12. Box plots of ACE with the  $p$  values of a one-sided  $t$  test that assesses the difference in the means of various ACE calculations.

of an upper bound of the impact that this could have, which is intentionally chosen to be overestimated. A one-sided  $t$  test yields a  $p$  value of 0.13, meaning that the difference is not significant at the 90 % level. Therefore, even if all tracks included TS-stage data due to some flaw in the algorithm, ACE would still be adequately represented. This is especially the case when considering that the presented scenario is inten-

tionally chosen to be an upper bound and that most TS-stage data truly reflect a TS in the data.

The results of Zarzycki and Ullrich (2017) show that ACE is less susceptible to changes when parameter thresholds are varied, which is comparable to the results presented here. Here, it is shown that ACE does not vary significantly when TD- and TS-stage systems are included or excluded. These systems are used to provide upper bounds for the impact of false positives and longer tails of tracks. It is suspected that the underlying reason is that ACE is dominated by intense TCs and that parameter threshold variation primarily affects weaker stages of TCs (as shown in Fig. 2). This hypothesis is supported by Bourdin et al. (2022), who reported that, in their comparison of different tracking schemes, strong cyclones are generally found by all compared schemes and weak cyclones are more susceptible to not being found by all.

Therefore, the impact of flaws in the tracking algorithm on ACE is concluded to be negligible, and the extension of the tail ends of tracks does not significantly increase the total energy produced throughout the full life cycle of individual TCs. The tracking algorithm is concluded to be capable of adequately capturing ACE within the underlying data.

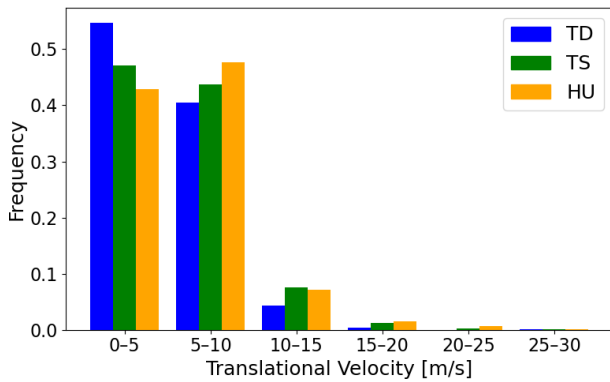


**Figure 13.** Normalized histogram of the translational velocity of HURDAT2 systems for tropical depressions (TDs, blue), tropical storms (TSs, green), and hurricanes (HUs, red).

## 8 Sensitivity to translational velocity

It has long been known that interaction with extratropical flow can accelerate the translational velocity of TCs undergoing ETT (e.g., Krueger, 1954; Palmén, 1958). This circumstance can accidentally, although conveniently, terminate TCs at some point during ETT via the maximum translational velocity criterion. This may cause the choice of the maximum translational velocity to be more impactful than intended. Therefore, the sensitivity to this threshold is investigated.

The maximum translational velocity threshold used for the preceding analyses is  $20 \text{ m s}^{-1}$ . Figure 13 shows histograms of the translational velocities of HURDAT2 systems of the TD, TS, and hurricane (HU) categories. This velocity is calculated as the great-circle distance between the TC's current location, where the categorization is made, and the location 6 h prior, divided by 6 h. Non-synoptic times are not considered.

The histograms show that it is extremely rare for observed TCs to move at a mean velocity of  $15 \text{ m s}^{-1}$  or faster. Thus, the TC tracking algorithm is applied three times, with the maximum allowed translational velocity set as 15, 20, and  $25 \text{ m s}^{-1}$ , respectively. Figure 14 shows the corresponding box plots. There is an increase in ACE with an increase in the maximum translational velocity, as a relaxation of this parameter naturally constructs longer tracks. However, with  $p$  values of 0.60 and 0.32 for the 15 and  $25 \text{ m s}^{-1}$  cases, respectively, there is no significant difference in the distribution of ACE. An increase in the maximum translational velocity inherently bears the risk of introducing erroneous tracking; therefore, an increase beyond  $20 \text{ m s}^{-1}$  does not seem necessary or appropriate. A reduction to  $15 \text{ m s}^{-1}$  appears to be feasible, but Fig. 13 shows that there are still a few observed TCs with a mean velocity above  $15 \text{ m s}^{-1}$ . Therefore, using  $20 \text{ m s}^{-1}$  appears to be the most appropriate maximum translational velocity.

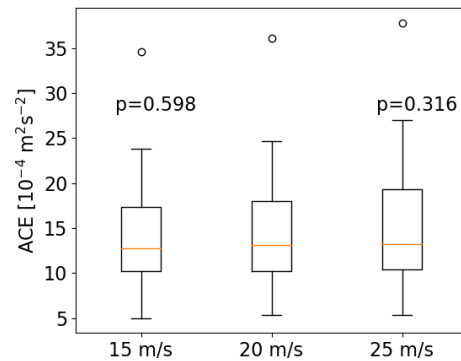


**Figure 14.** Box plots of ACE with the  $p$  values of a one-sided  $t$  test that assesses the difference in the means of ACE using different maximum translational velocities.

## 9 Conclusions

A tracking algorithm for tropical cyclones was developed for use with ICON output data. The algorithm successfully tracks systems with the following strengths: tropical depression, tropical storm, and hurricane. About 36 % of TC tracks begin with a strong central vorticity maximum, and about 34 % begin with an aggregation of multiple vorticity maxima, in line with the VHT theory of TC cyclogenesis (Montgomery and Smith, 2014). About 19 % of TC tracks begin with an ongoing aggregation process and remain within this process for at least the first 24 h. About 12 % of tracked systems are false positives.

The benefit of threshold parameter variation is apparent in the tracking of weak systems, especially at early stages of the TC life cycle. In particular, the relaxation of the warm-core criterion allows for a larger distance between the warm-core temperature anomaly maximum and the sea level pressure minimum. This distance becoming too large is the leading cause of track termination in TCs that are weak but could feasibly be tracked for longer. However, it also allows for structures that are not warm cores to be falsely tracked. This is evident not only from the approximate 12 % of false positives but also from the TC termination, where a wrongful continuation of a system can be tracked. As the use of the OWZ parameter is particularly useful in detecting cyclogenesis, a comparison between the threshold parameter variation and the OWZ parameter for tracking early stages of a TC may be in order. Joint use of the two methods could be feasible. Variations in the vorticity threshold do not seem to be of much importance, as TCs that are tracked typically fulfill even the most strict vorticity criterion. A threshold of  $10^{-6} \text{ s}^{-1}$  could, thus, be sufficient, as this constrains the resulting tracks to those with positive vorticity.

Specifically for weak TCs, the maximum wind speed is often underestimated. This is because they often have a radius of maximum winds that is larger than the maximum radius within which the algorithm determines maximum wind

speeds. An increase in radius may provide more accurate results, although care needs to be taken to not accidentally include winds that are not part of the TC. It is possible that using a variable radius threshold based on central pressure could be beneficial, as weak TCs in particular are affected. However, a more accurate detection of TC genesis should precede this to provide a more solid basis for the exact nature of the radius variability.

The warm-core criteria are central to discriminating between TCs and other low-pressure systems. They are also responsible for most track terminations. Therefore, these criteria in particular need to be refined. Within the dataset used, strong environmental temperature gradients have caused the warm-core criteria to be fulfilled even in the absence of a warm core. A possible solution to this would be to not only use the environmental mean temperature as a reference but also to introduce an additional requirement of having to reach a minimum positive anomaly within every quadrant. This would cause the criterion to not be fulfilled when one side of the detected system is substantially warmer than the other side, i.e., when a strong environmental gradient is present. Furthermore, the offset of the temperature anomaly maximum from the pressure minimum could be treated explicitly. This could consist of introducing a new threshold parameter that determines the maximal allowed distance between the two extrema and that could be made dependent on the central pressure, as this is particularly relevant for weak systems.

While cyclones could be detected and tracked by a dedicated algorithm for extratropical cyclones after the transition, there is no guarantee that this does not result in gaps between the tropical and extratropical stage of cyclones during the transition. Therefore, a further possible addition to the algorithm would be an explicit treatment of ETT. Currently, this process is only included via the warm-core criteria, which is not only immensely inelegant but also allows for no control over how this process is tracked. A clear definition of the transition process is given in Evans and Hart (2003), and Bieli et al. (2020) and Bourdin et al. (2022) both provide useful methods to implement this capability.

Furthermore, the effect of tracking errors on ACE has been investigated. The false positives appear to only have a minor impact on ACE. A hypothetical case where all detections of TD- and TS-strength systems are false is used to show that, even if this were the case, the impact on ACE would be insignificant. Therefore, the ACE value calculated from the tracking algorithm output is concluded to reflect the true ACE value within the simulation data. Thus, changes to how cyclogenesis is being tracked can be made without substantially impacting ACE. Explicit treatment of the ETT process might have a larger impact, as these systems can still have somewhat high wind speeds and ETT occurs frequently.

*Code and data availability.* The code of the tracking algorithm and the data used for the production of this paper are published on

Zenodo at <https://doi.org/10.5281/zenodo.7331861> (Enz and Engelmann, 2022) and <https://doi.org/10.5281/zenodo.8190691> (Enz, 2023), respectively.

*Author contributions.* JPE wrote the tracking algorithm and performed a first validation thereof, which is not part of this study. BME supervised this work and performed the validation presented here as part of his PhD thesis under the supervision of UL. All the authors contributed to the manuscript.

*Competing interests.* The contact author has declared that none of the authors has any competing interests.

*Disclaimer.* Publisher's note: Copernicus Publications remains neutral with regard to jurisdictional claims in published maps and institutional affiliations.

*Acknowledgements.* The authors thank the three anonymous reviewers for their feedback, which has been used to improve the quality of the paper.

*Review statement.* This paper was edited by Chanh Kieu and reviewed by three anonymous referees.

## References

- Bechtold, P., Köhler, M., Jung, T., Doblas-Reyes, F., Leutbecher, M., Rodwell, M. J., Vitart, F., and Balsamo, G.: Advances in simulating atmospheric variability with the ECMWF model: From synoptic to decadal time-scales, *Q. J. Roy. Meteorol. Soc.*, 134, 1337–1351, <https://doi.org/10.1002/qj.289>, 2008.
- Bell, G. D., Halpert, M. S., Schnell, R. C., Higgins, R. W., Lawrimore, J., Kousky, V. E., Tinker, R., Thiaw, W., Cheliah, M., and Artusa, A.: Climate Assessment for 1999, *B. Am. Meteorol. Soc.*, 81, S1–S50, [https://doi.org/10.1175/1520-0477\(2000\)81\[s1:CAF\]2.0.CO;2](https://doi.org/10.1175/1520-0477(2000)81[s1:CAF]2.0.CO;2), 2000.
- Bell, S. S., Chand, S. S., Tory, K. J., and Turville, C.: Statistical Assessment of the OWZ Tropical Cyclone Tracking Scheme in ERA-Interim, *J. Climate*, 31, 2217–2232, <https://doi.org/10.1175/JCLI-D-17-0548.1>, 2018.
- Bender, M. A., Knutson, T. R., Tuleya, R. E., Sirutis, J. J., Vecchi, G. A., Garner, S. T., and Held, I. M.: Modeled Impact of Anthropogenic Warming on the Frequency of Intense Atlantic Hurricanes, *Science*, 327, 454–458, <https://doi.org/10.1126/science.1180568>, 2010.
- Bengtsson, L., Botzet, M., and Esch, M.: Hurricane-type vortices in a general circulation model, *Tellus A*, 47, 175–196, <https://doi.org/10.1034/j.1600-0870.1995.t01-1-00003.x>, 1995.
- Bieli, M., Sobel, A. H., Camargo, S. J., Murakami, H., and Vecchi, G. A.: Application of the Cyclone Phase Space to Extratropical Transition in a Global Climate Model, *J. Adv. Model. Earth Sy.*,

- 12, e2019MS001878, <https://doi.org/10.1029/2019MS001878>, 2020.
- Bourdin, S., Fromang, S., Dulac, W., Cattiaux, J., and Chauvin, F.: Intercomparison of four algorithms for detecting tropical cyclones using ERA5, *Geosci. Model Dev.*, 15, 6759–6786, <https://doi.org/10.5194/gmd-15-6759-2022>, 2022.
- Camargo, S. J. and Zebiak, S. E.: Improving the detection and tracking of tropical cyclones in atmospheric general circulation models, *Weather Forecast.*, 17, 1152–1162, [https://doi.org/10.1175/1520-0434\(2002\)017<1152:ITDATO>2.0.CO;2](https://doi.org/10.1175/1520-0434(2002)017<1152:ITDATO>2.0.CO;2), 2002.
- Chauvin, F., Royer, J.-F., and Déqué, M.: Response of hurricane-type vortices to global warming as simulated by ARPEGE-Climat at high resolution, *Clim. Dynam.*, 27, 377–399, <https://doi.org/10.1007/s00382-006-0135-7>, 2006.
- Davis, C. A. and Bosart, L. F.: Baroclinically Induced Tropical Cyclogenesis, *Mon. Weather Rev.*, 131, 2730–2747, [https://doi.org/10.1175/1520-0493\(2003\)131<2730:BITC>2.0.CO;2](https://doi.org/10.1175/1520-0493(2003)131<2730:BITC>2.0.CO;2), 2003.
- Davis, C. A. and Bosart, L. F.: The TT Problem: Forecasting the Tropical Transition of Cyclones, *B. Am. Meteorol. Soc.*, 85, 1657–1662, 2004.
- Durden, S. L.: Observed tropical cyclone eye thermal anomaly profiles extending above 300 hPa, *Mon. Weather Rev.*, 141, 4256–4268, <https://doi.org/10.1175/MWR-D-13-00021.1>, 2013.
- Enz, B.: Data Used for the Publication “Use of Threshold Parameter Variation for Tropical Cyclone Tracking”, Zenodo [data set], <https://doi.org/10.5281/zenodo.8190691>, 2023.
- Enz, B. and Engelmann, J.: TC Tracking Algorithm for Use with ICON, Zenodo [code], <https://doi.org/10.5281/zenodo.7331861>, 2022.
- Evans, J. L. and Hart, R. E.: Objective indicators of the life cycle evolution of extratropical transition for atlantic tropical cyclones, *Mon. Weather Rev.*, 131, 909–925, [https://doi.org/10.1175/1520-0493\(2003\)131<0909:OIOTLC>2.0.CO;2](https://doi.org/10.1175/1520-0493(2003)131<0909:OIOTLC>2.0.CO;2), 2003.
- Gentry, M. S. and Lackmann, G. M.: Sensitivity of simulated tropical cyclone structure and intensity to horizontal resolution, *Mon. Weather Rev.*, 138, 688–704, <https://doi.org/10.1175/2009MWR2976.1>, 2010.
- Grinsted, A., Ditlevsen, P., and Christensen, J. H.: Normalized US hurricane damage estimates using area of total destruction, 1900–2018, *P. Natl. Acad. Sci. USA*, 116, 23942–23946, <https://doi.org/10.1073/pnas.1912277116>, 2019.
- Hart, R. E. and Evans, J. L.: A climatology of the extratropical transition of Atlantic tropical cyclones, *J. Climate*, 14, 546–564, [https://doi.org/10.1175/1520-0442\(2001\)014<0546:ACOTET>2.0.CO;2](https://doi.org/10.1175/1520-0442(2001)014<0546:ACOTET>2.0.CO;2), 2001.
- Hersbach, H., Bell, B., Berrisford, P., Hirahara, S., Horányi, A., Muñoz-Sabater, J., Nicolas, J., Peubey, C., Radu, R., Schepers, D., Simmons, A., Soci, C., Abdalla, S., Abellan, X., Balsamo, G., Bechtold, P., Biavati, G., Bidlot, J., Bonavita, M., De Chiara, G., Dahlgren, P., Dee, D., Diamantakis, M., Dragani, R., Fleming, J., Forbes, R., Fuentes, M., Geer, A., Haimberger, L., Healy, S., Hogan, R. J., Hólm, E., Janisková, M., Keeley, S., Laloyaux, P., Lopez, P., Lupu, C., Radnoti, G., de Rosnay, P., Rozum, I., Vamborg, F., Villaume, S., and Thépaut, J.-N.: The ERA5 global reanalysis, *Q. J. Roy. Meteor. Soc.*, 146, 1999–2049, <https://doi.org/10.1002/qj.3803>, 2020.
- Hodges, K. I.: Adaptive Constraints for Feature Tracking, *Mon. Weather Rev.*, 127, 1362–1373, [https://doi.org/10.1175/1520-0493\(1999\)127<1362:ACFFT>2.0.CO;2](https://doi.org/10.1175/1520-0493(1999)127<1362:ACFFT>2.0.CO;2), 1999.
- Horn, M., Walsh, K., Zhao, M., Camargo, S. J., Scoccimarro, E., Murakami, H., Wang, H., Ballinger, A., Kumar, A., Shaevitz, D. A., Jonas, J. A., and Oouchi, K.: Tracking scheme dependence of simulated tropical cyclone response to idealized climate simulations, *J. Climate*, 27, 9197–9213, <https://doi.org/10.1175/JCLI-D-14-00200.1>, 2014.
- Kleppeck, S., Muccione, V., Raible, C. C., Bresch, D. N., Koellner-Heck, P., and Stocker, T. F.: Tropical cyclones in ERA-40: A detection and tracking method, *Geophys. Res. Lett.*, 35, L10705, <https://doi.org/10.1029/2008GL033880>, 2008.
- Krueger, A. F.: The weather and circulation of October 1954, *Mon. Weather Rev.*, 82, 296–300, 1954.
- Landsea, C. W. and Franklin, J. L.: Atlantic Hurricane Database Uncertainty and Presentation of a New Database Format, *Mon. Weather Rev.*, 141, 3576–3592, <https://doi.org/10.1175/MWR-D-12-00254.1>, 2013.
- McTaggart-Cowan, R., Galarneau, T. J., Bosart, L. F., Moore, R. W., and Martius, O.: A Global Climatology of Baroclinically Influenced Tropical Cyclogenesis, *Mon. Weather Rev.*, 141, 1963–1989, <https://doi.org/10.1175/MWR-D-12-00186.1>, 2013.
- McTaggart-Cowan, R., Davies, E. L., Fairman, J. G., Galarneau, T. J., and Schultz, D. M.: Revisiting the 26.5°C sea surface temperature threshold for tropical cyclone development, *B. Am. Meteorol. Soc.*, 96, 1929–1943, <https://doi.org/10.1175/BAMS-D-13-00254.1>, 2015.
- Montgomery, M. T. and Smith, R. K.: Paradigms for tropical cyclone intensification, *Aust. Meteorol. Ocean.*, 64, 37–66, 2014.
- Montgomery, M. T. and Smith, R. K.: Recent Developments in the Fluid Dynamics of Tropical Cyclones, *Annu. Rev. Fluid Mech.*, 49, 541–574, <https://doi.org/10.1146/annurev-fluid-010816-060022>, 2017.
- Okubo, A.: Horizontal dispersion of floatable particles in the vicinity of velocity singularities such as convergences, *Deep-Sea Res.*, 17, 445–454, [https://doi.org/10.1016/0011-7471\(70\)90059-8](https://doi.org/10.1016/0011-7471(70)90059-8), 1970.
- Ooyama, K.: Numerical Simulation of the Life Cycle of Tropical Cyclones, *J. Atmos. Sci.*, 26, 3–40, [https://doi.org/10.1175/1520-0469\(1969\)026<0003:NSOTLC>2.0.CO;2](https://doi.org/10.1175/1520-0469(1969)026<0003:NSOTLC>2.0.CO;2), 1969.
- Palmen, E.: On the formation and structure of tropical hurricanes, *Geophysica*, 3, 26–38, 1948.
- Palmén, E.: Vertical Circulation and Release of Kinetic Energy during the Development of Hurricane Hazel into an Extratropical Storm, *Tellus*, 10, 1–13, <https://doi.org/10.3402/tellusa.v10i1.9222>, 1958.
- Pielke Jr., R. A., Gratz, J., Landsea, C. W., Collins, D., Saunders, M. A., and Musulin, R.: Normalized Hurricane Damage in the United States: 1900–2005, *Nat. Hazards Rev.*, 9, 29–42, [https://doi.org/10.1061/\(ASCE\)1527-6988\(2008\)9:1\(29\)](https://doi.org/10.1061/(ASCE)1527-6988(2008)9:1(29)), 2008.
- Saffir, H. S.: Hurricane wind and storm surge, *The Military Engineer*, 65, 4–5, 1973.
- Smith, R. K. and Montgomery, M. T.: Toward clarity on understanding tropical cyclone intensification, *J. Atmos. Sci.*, 72, 3020–3031, <https://doi.org/10.1175/JAS-D-15-0017.1>, 2015.
- Stern, D. P. and Nolan, D. S.: On the Height of the Warm Core in Tropical Cyclones, *J. Atmos. Sci.*, 69, 1657–1680, <https://doi.org/10.1175/JAS-D-11-010.1>, 2012.

- Strachan, J., Vidale, P. L., Hodges, K., Roberts, M., and Demory, M.-E.: Investigating Global Tropical Cyclone Activity with a Hierarchy of AGCMs: The Role of Model Resolution, *J. Climate*, 26, 133–152, <https://doi.org/10.1175/JCLI-D-12-00012.1>, 2013.
- Tory, K. J., Dare, R. A., Davidson, N. E., McBride, J. L., and Chand, S. S.: The importance of low-deformation vorticity in tropical cyclone formation, *Atmos. Chem. Phys.*, 13, 2115–2132, <https://doi.org/10.5194/acp-13-2115-2013>, 2013.
- Tsutsui, J.-I. and Kasahara, A.: Simulated tropical cyclones using the National Center for Atmospheric Research community climate model, *J. Geophys. Res.-Atmos.*, 101, 15013–15032, <https://doi.org/10.1029/95JD03774>, 1996.
- Ullrich, P. A. and Zarzycki, C. M.: TempestExtremes: a framework for scale-insensitive pointwise feature tracking on unstructured grids, *Geosci. Model Dev.*, 10, 1069–1090, <https://doi.org/10.5194/gmd-10-1069-2017>, 2017.
- Walsh, K., Lavender, S., Scoccimarro, E., and Murakami, H.: Resolution dependence of tropical cyclone formation in CMIP3 and finer resolution models, *Clim. Dynam.*, 40, 585–599, <https://doi.org/10.1007/s00382-012-1298-z>, 2012.
- Walsh, K. J. E., Fiorino, M., Landsea, C. W., and McInnes, K. L.: Objectively Determined Resolution-Dependent Threshold Criteria for the Detection of Tropical Cyclones in Climate Models and Reanalyses, *J. Climate*, 20, 2307–2314, <https://doi.org/10.1175/JCLI4074.1>, 2007.
- Wang, X. and Jiang, H.: A 13-Year Global Climatology of Tropical Cyclone Warm-Core Structures from AIRS Data, *Mon. Weather Rev.*, 147, 773–790, <https://doi.org/10.1175/MWR-D-18-0276.1>, 2019.
- Weiss, J.: The dynamics of enstrophy transfer in two-dimensional hydrodynamics, *Physica D*, 48, 273–294, [https://doi.org/10.1016/0167-2789\(91\)90088-Q](https://doi.org/10.1016/0167-2789(91)90088-Q), 1991.
- Willoughby, H. M.: The Dynamics of the Tropical Cyclone Core, *Aust. Meteorol. Mag.*, 36, 183–191, 1988.
- Zängl, G., Reinert, D., Rípodas, P., and Baldauf, M.: The ICON (ICOsahedral Non-hydrostatic) modelling framework of DWD and MPI-M: Description of the non-hydrostatic dynamical core, *Q. J. Roy. Meteor. Soc.*, 141, 563–579, <https://doi.org/10.1002/qj.2378>, 2015.
- Zarzycki, C. M. and Ullrich, P. A.: Assessing sensitivities in algorithmic detection of tropical cyclones in climate data, *Geophys. Res. Lett.*, 44, 1141–1149, <https://doi.org/10.1002/2016GL071606>, 2017.
- Zhang, G., Wang, Z., Dunkerton, T. J., Peng, M. S., and Magnusdotir, G.: Extratropical Impacts on Atlantic Tropical Cyclone Activity, *J. Atmos. Sci.*, 73, 1401–1418, <https://doi.org/10.1175/JAS-D-15-0154.1>, 2016.
- Zhao, M., Held, I. M., Lin, S.-J., and Vecchi, G. A.: Simulations of global hurricane climatology, interannual variability, and response to global warming using a 50-km resolution GCM, *J. Climate*, 22, 6653–6678, <https://doi.org/10.1175/2009JCLI3049.1>, 2009.